




# Thermally conductive poly(ether ether ketone)/boron nitride composites with low coefficient of thermal expansion

Barun Ghosh<sup>1</sup>, Fang Xu<sup>1,\*</sup> , and Xianghui Hou<sup>1</sup>

<sup>1</sup> Faculty of Engineering, Advanced Materials Research Group, University of Nottingham, Nottingham NG7 2RD, UK

Received: 15 November 2020

Accepted: 8 February 2021

© Crown 2021

## ABSTRACT

The substantial heat generation due to miniaturization and high-degree integration of electronic devices is one of the major issues to facilitate efficient thermal management in power electronics. Though epoxy-based composites have shown great interest in different applications such as laminated circuit board, electronic component encapsulations, and potting, they have low application temperature (up to 150 °C) and higher mismatch of coefficient of thermal expansion (CTE) between the heat source and heat sink. Here, poly(ether ether ketone) (PEEK) composites reinforced with hexagonal boron nitride (hBN) nanoplatelets have been developed by liquid mixing and re-melting method for a step change in composite materials with lower CTE and significantly improved thermal dissipation capability. The lowest achieved CTE is  $2.1 \mu\text{m m}^{-1} \text{K}^{-1}$ , and the highest thermal conductivity is  $1.04 \text{ W m}^{-1} \text{K}^{-1}$  in PEEK/hBN composites at 30 wt% hybrid hBN content (hBN platelets with two different sizes, i.e. 70 nm and 500 nm, taken as 1:1 weight ratio), due to the formation of thermally conductive inter-filler networks. The composites show negligible variation in  $K$  with the working temperature up to 250 °C. The developed composites also exhibit excellent electrical insulation properties; thus, they will have good potential in thermal management for power electronic applications.

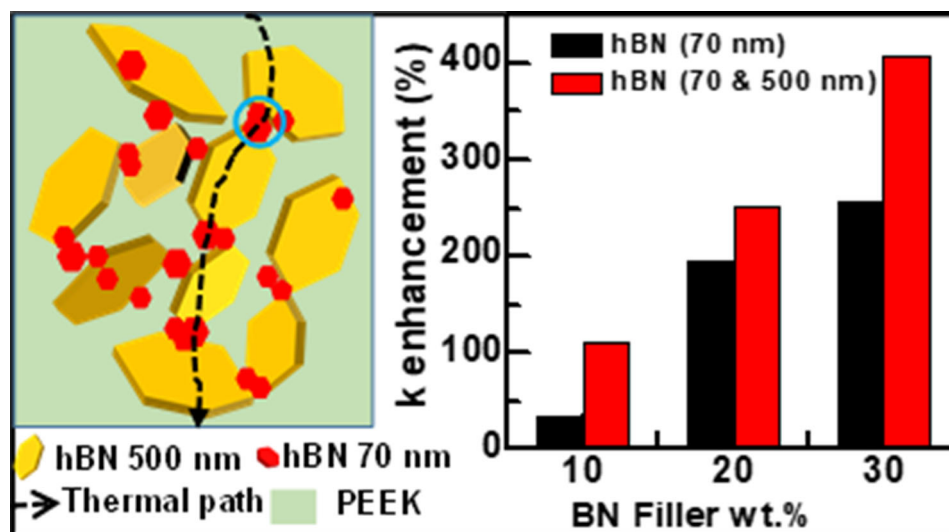
Handling Editor: Gregory Rutledge.

Address correspondence to E-mail: Fang.Xu@nottingham.ac.uk

<https://doi.org/10.1007/s10853-021-05923-0>

Published online: 05 March 2021

## GRAPHICAL ABSTRACT



## Introduction

The continuing miniaturization and increasing power output of electronic devices have created several challenges in thermal management and electronic packaging. High thermal conductivity, along with low CTE and high electrical insulation, is required for a high-density electrical power system. The existing materials for printed circuit board (PCB) are mainly based on glass fibre reinforced epoxy resin (FR4). However, FR4 experiences a very low thermal conductivity ( $0.16\text{--}0.26\text{ W m}^{-1}\text{ K}^{-1}$ ) along with a large difference in CTE towards X–Y and Z direction ( $16\text{ }\mu\text{m m}^{-1}\text{ K}^{-1}$  along X–Y direction and  $54\text{--}60\text{ }\mu\text{m m}^{-1}\text{ K}^{-1}$  along Z direction) due to the two-dimensional distribution of glass fibres inside the resin [1]. Efficient cooling of electronic devices requires minimal CTE mismatch between the heat source and heat sink. A large difference in the CTEs often causes mechanical stresses, which would seriously affect the device reliability [2]. Nowadays, silicon is used as heat source, and copper or aluminium is used as heat-dissipating materials, which show a large CTE mismatch with silicon and cannot directly attach to a silicon surface without stress compensating interlayers. Thus, the development of an

alternative to FR4 becomes hot anvil. Materials with high  $K$  and minimum CTE mismatch between the heat source and heat sink are in great demand for electronic packaging applications. Polymer composites reinforcing with highly thermal conducting inorganic fillers have attracted increasing attention in this field [3–7]. Though pure polymers have very low thermal conductivity ( $0.1\text{--}0.3\text{ W m}^{-1}\text{ K}^{-1}$ ), controlling such inorganic fillers in the polymer matrix can significantly increase the thermal conductivity and reduce the CTE along all directions, which will meet the requirement for thermal management and electronic packaging applications.

PEEK has emerged as a high-performance engineering material with excellent mechanical strength, incomparable chemical resistance, good thermal stabilities, wear resistance, and biocompatibility [8]. Incorporation of inorganic nanoparticles into the PEEK matrix can significantly improve the mechanical properties [9, 10], thermal stability [11, 12], thermal conductivity [13, 14], and tribological properties [15, 16] of the composites. With the modulus of 3.2 GPa and working temperature up to 260 °C, PEEK is considered as an advanced material in the electronic, machinery, aerospace, and automotive industries [17, 18]. PEEK nanocomposites have also been considered as membrane for polymer electrolyte fuel cell

applications [19–22]. PEEK has thermal conductivity of  $0.20 \text{ W m}^{-1} \text{ K}^{-1}$ , glass transition temperature ( $T_g$ )  $\sim 145 \text{ }^\circ\text{C}$  and CTE  $47 \text{ } \mu\text{m m}^{-1} \text{ K}^{-1}$  [23]. Among the different inorganic fillers, hexagonal boron nitride (hBN) has attracted much attention due to their high-temperature stability, low dielectric constant, high electrical insulation, high heat and chemical resistance, good mechanical properties and extremely high thermal conductivity ( $300 \text{ W m}^{-1} \text{ K}^{-1}$  for in-plane direction,  $K_{//}$  and  $30 \text{ W m}^{-1} \text{ K}^{-1}$  along through-plane direction,  $K_{\perp}$ ) with very low CTE ( $1.1\text{--}4.3 \text{ } \mu\text{m m}^{-1} \text{ K}^{-1}$ ) [24–28]. Due to its higher thermal conductivity, which is even much higher than other inorganic fillers such as aluminium nitride (AlN,  $K \sim 150\text{--}220 \text{ W m}^{-1} \text{ K}^{-1}$  and CTE  $\sim 2.5\text{--}5 \text{ } \mu\text{m m}^{-1} \text{ K}^{-1}$ ), aluminium oxide ( $\text{Al}_2\text{O}_3$ ,  $K \sim 38\text{--}42 \text{ W m}^{-1} \text{ K}^{-1}$  and CTE  $\sim 7 \text{ } \mu\text{m m}^{-1} \text{ K}^{-1}$ ), silicon nitride ( $\text{Si}_3\text{N}_4$ ,  $K \sim 86\text{--}120 \text{ W m}^{-1} \text{ K}^{-1}$  and CTE  $\sim 2.7\text{--}3.1 \text{ } \mu\text{m m}^{-1} \text{ K}^{-1}$ ), and silicon carbide (SiC,  $K \sim 85 \text{ W m}^{-1} \text{ K}^{-1}$  and CTE  $\sim 4.1\text{--}4.7 \text{ } \mu\text{m m}^{-1} \text{ K}^{-1}$ ) [7], incorporation of hBN nanoplatelets into the PEEK can significantly increase the thermal conductivity, as well as lowering the CTE of the composites, which is required for the next-generation power electronic applications. The development of PEEK/hBN composites could potentially replace the glass fibre reinforced epoxy composites to avoid an undesirable CTE along Z direction, thus an isotropic CTE and improved thermal conductivity could be achieved.

The use of thermally conductive hybrid filler (different shapes or types) into polymer matrix is an effective approach to increase the thermal conductivity of the composites. By adding hybrid fillers, the composites would have better thermal conductivities than those with single type of thermally conductive fillers due to the enhanced connectivity offered by structuring fillers with high aspect ratio in hybrid fillers [29]. Hybrid fillers can improve the dispersion performance of the fillers in polymer matrix and help to bridge the adjacent fillers to form enhanced thermal conduction paths/channels [30]. Some common hybrid fillers used to prepare the high thermal conductive composites are binary hybrids such as SiCw/SiCp [31],  $\mu\text{BN/nBN}$  [32], MWCNT/ $\text{Al}_2\text{O}_3$  [33], graphene/CNT [34], and multi-hybrids such as BN/GNPs/CF [35] and CF/hBN/Cu [36].

In this present work, we have investigated the effect of nano hBN loadings, and hybrid fillers with different hBN sizes (70 nm and 500 nm) on the

thermal conductivity and CTE of PEEK/hBN composites. The surface morphology, microstructural features, and thermogravimetric analysis were also studied for these PEEK/hBN composites with different filler loadings. The interfacial thermal resistance of the composites was calculated based on the effective medium theory (EMT) model and compared with the experimental results to explain the enhancement in thermal conductivity.

## Experimental details

### Materials

hBN nanoparticles with average diameter  $\sim 70 \text{ nm}$  and  $\sim 500 \text{ nm}$  were purchased from M.K. Impex Corp. 704 PEEK powder was ordered from VICTREX PEEK Polymer Ltd, UK. Analytical grade (99.99%) isopropyl alcohol (IPA) and acetone (Fisher Scientific, UK) were used for the dispersion of PEEK and hBN nanoparticles.

### Composites fabrication

The PEEK/hBN composites were prepared by liquid mixing and re-melting. Solution mixing is the most straightforward fabrication technique for polymer nanocomposites [37]. In this process, nanofillers are first solved in certain solvents followed by the simple mixing of polymer and nanofiller dispersions. The dispersion of nanofillers in polymer matrices is facilitated by the ultrasonication, which applies the ultrasonic energy to the nanofiller bundles/agglomerates. The agglomerates are agitated when ultrasound passes through in the form of high-frequency waves. These waves produce higher energy than the interaction energy between nanofillers in agglomerates, which leads to the separation of the individual particle from the agglomerates. Here in our work, firstly, a volume ratio (1:1) of isopropyl alcohol and distilled water was used to disperse the PEEK powder and hBN nanopowder ( $\sim 70 \text{ nm}$ ) at different concentrations (5 wt%, 7 wt%, 10 wt%, and 15 wt%, 20 wt%, and 30 wt%). hBN and PEEK powders were separately dispersed in 100 ml of the isopropyl alcohol–water solution, followed by vigorous magnetic stirring for 1 h. Then, these two well-dispersed suspensions were mixed using the ultrasonic probe treatment for 30 min, followed by a further 1 h

vigorous magnetic stirring to mix the solution. Then, the mixture was heated on a hot plate at 120 °C under continuous stirring to remove the solvent. The resulting powders were dried in an oven at 120 °C overnight, to remove the solvent completely. The mixed powders of PEEK and hBN were then transferred onto a stain steel mould. It was then kept in a furnace at 400 °C for 15 min to melt the powder. A mould releasing agent was also sprayed so that the composite can be easily peeled off after cooling. Similarly, in the case of hybrid fillers, 500 nm hBN nanoplatelets were mixed with 70 nm hBN by 1:1 weight ratio, and then the remaining process for the preparation of the composites was similar. We have used a maximum of 30 wt% hBN concentration to prepare the composites. A higher concentration of hBN (more than 30 wt%) requires a furnace temperature higher than 400 °C to completely melt the mixed powders of PEEK and hBN and also there is a probability to increase the melting viscosity at higher concentrations which will, in turn, increase the number of voids inside the composite. Finally, the composites were polished to smooth the surface for characterizations.

### Microstructural and thermal and electrical analysis

Scanning electron micrographs were obtained using a JEOL 7100F field-emission gun scanning electron microscope (FEG-SEM). A working distance of 10 mm was maintained utilizing a beam voltage of 10 kV. Crystallographic structures were assessed using a Bruker D8 advance XRD spectrometer, utilizing a parallel beam geometry and glancing angle beam parameters as follows: Cu K $\alpha$  source;  $\lambda = 1.5406 \text{ \AA}$ ; 40 kV; 35 mA. Diffraction patterns were recorded over a  $2\theta$  range of 10°–60°, with a step size of 0.015° ( $2\theta$ ). The Fourier transform infrared spectra were obtained from a Thermo Fisher Scientific Nicolet IR machine. Thermogravimetric analyses (TGA) were carried out using approximately 10 mg powder using a TA-SDT Q600 machine, from room temperature to 800 °C at a heating rate of 10 °C min<sup>-1</sup> under an airflow of 100 cm<sup>3</sup> min<sup>-1</sup> to determine different thermal parameters ( $T_{onset}$ ,  $T_{max}$ ,  $T_m$ ,  $\Delta H_m$ ,  $X_c$ , and  $T_g$ ) of the pure polymer and the composites. A blank run was carried out to determine the baseline, which was then subtracted from the plot

obtained using TA universal analysis 2000 software. The coefficient of thermal expansion of the composites was measured using thermomechanical analyzer (TMA) (model no. Q400 TMA) with a preloaded force of 0.02 N with a 5 °C min<sup>-1</sup> heating rate. A NETZSCH LFA 467 HyperFlash facility was used to determine the thermal conductivity of the composites from 25 °C to 250 °C, using a specimen size of 10 mm  $\times$  10 mm and a thickness of ca. 2.5 mm by the following equation:

$$K = \alpha \cdot C_p \cdot d \quad (1)$$

where  $\alpha$  is the thermal diffusivity,  $C_p$  is the specific heat measured from differential scanning calorimetry (DSC model no: TA DSC2500), and  $d$  is the density of the composite calculated from the Archimedes' principle. The interfacial thermal resistance was estimated by introducing effective medium theory (EMT) model to fit the experimental data using the following equations [38]:

$$K = K_m \frac{3 + V_f(\beta_1 + \beta_2)}{3 - V_f\beta_1} \quad (2)$$

$$\beta_1 = \frac{2[d(K_{BN} - K_m) - 2R_k K_m K_{BN}]}{d(K_{BN} + K_m) + 2R_k K_m K_{BN}} \quad (3)$$

where  $K$  is the thermal conductivity of the composite.  $K_m$  and  $K_{BN}$  represent the thermal conductivity of PEEK matrix (0.20 W m<sup>-1</sup> K<sup>-1</sup>) and pure hBN platelets (300 W m<sup>-1</sup> K<sup>-1</sup>), respectively.  $V_f$  is the volume fraction, and  $d$  (15 nm) is the thickness of hBN platelets. The volume resistivity of the composite was measured by Keithley 6517B Electrometer. Volume resistivity is the impedance of a material per unit volume to current, and it is used to characterize the electrical properties of a material. A flat sample of 2.5 mm thickness was placed between two electrodes, and measure the direct-current voltage applied to the electrode and the current flowing through the volume of the sample and then, dividing the two values, the volume resistivity of the composite was obtained.

### Results and discussion

Figure 1a, b show the scanning electron microscopy (SEM) images of mixed powders of 15 wt% hBN ( $\sim 70 \text{ nm}$ ) in PEEK at different magnification. The hexagonal BN nanoplatelets are clearly observed and



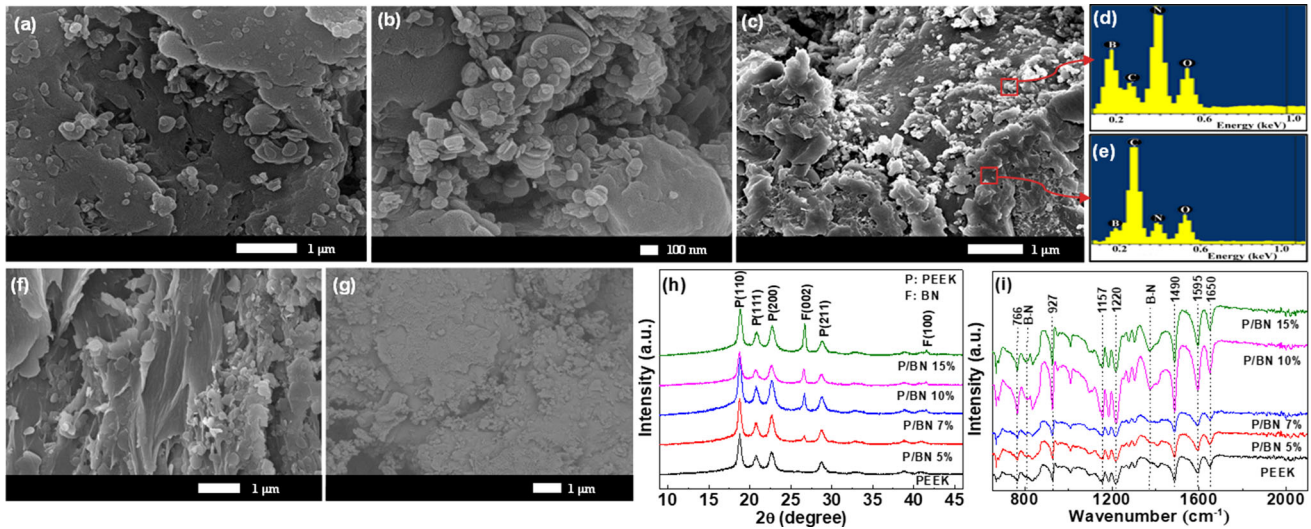


**Figure 1** (a, b) SEM images of mixed powders of 15 wt% hBN ( $\sim 70$  nm) in PEEK at two different magnification. (c, f) Cross-sectional SEM images of the PEEK/hBN (15 wt%) bulk composite. (g) Cross-sectional SEM image of the same bulk composite at backscattered electron (BSE) mode. EDS spectra of

the two different regions of the bulk composite shown as red squares in (c): **d** filler region, and **e** polymer matrix region. **h** XRD patterns and **i** FTIR spectra of pure PEEK and the PEEK/hBN composites with different hBN loadings.

mixed well with the polymer matrix. The hBN nanoparticles are also randomly distributed throughout the polymer matrix even after melting the mixed powders to get the bulk composite, which is shown as cross-sectional SEM images in Fig. 1c, f. Figure 1g shows the cross-sectional image of the bulk composite at backscattered electron (BSE) mode, confirming the well distributed hBN particles throughout the PEEK matrix. Two typical regions of hBN filler and PEEK matrix are highlighted as red squares in the SEM image of Fig. 1c and their corresponding energy-dispersive X-ray spectra (EDS) are shown in Fig. 1d and Fig. 1e, respectively. The nanoparticles appeared to be well distributed within the matrix and looked consistently homogenous. The X-ray diffraction (XRD) patterns of pure PEEK and the PEEK/hBN composites with different hBN loadings ( $\sim 70$  nm) are shown in Fig. 1h. Pure PEEK crystallizes primarily in the orthorhombic form showing diffraction peaks corresponding to the reflection from (110), (111), (200), and (211) planes [39]. The composites with different filler loadings show additional diffraction peaks of hexagonal hBN at  $2\theta$  of  $26.6^\circ$  and  $41.6^\circ$  corresponding to the reflection from (002) and (100) plane, respectively, indicating the phase of hBN nanoparticles remains unchanged inside the PEEK matrix.

The interaction between the nanoparticles and polymer matrix was also investigated using Fourier transform infrared spectra (FTIR) analysis. Figure 1i shows the FTIR spectra of pure PEEK and the PEEK/hBN composites at different hBN loadings ( $\sim 70$  nm). The hBN features are reflected at  $1374\text{ cm}^{-1}$  and  $809\text{ cm}^{-1}$ , corresponding to B-N stretching vibration and the B-N-B out-of-plane bending vibration modes, respectively. The peaks at  $1650\text{ cm}^{-1}$  and  $1220\text{ cm}^{-1}$  belong to the keto group, while the peaks at  $1595\text{ cm}^{-1}$  and  $1490\text{ cm}^{-1}$  are due to the C-H band of in-plane bending benzene vibration. The additional peaks at  $927\text{ cm}^{-1}$  and  $766\text{ cm}^{-1}$  are assigned to the out-of-plane bending vibration of the benzene ring [16]. These similar FTIR spectra indicate that the original PEEK structure was unchanged by the inclusion of hBN nanoparticles.

The thermal stability of the PEEK/hBN composites along with pure PEEK is shown in Fig. 2a, and their corresponding differential scanning calorimetry (DSC) curves around the melting point are presented in Fig. 2b. The key thermal parameters obtained from the measurement are listed in Table 1.  $T_{onset}$  represents the onset temperature of the degradation, and  $T_{max}$  refers to the temperature at the maximum rate of degradation. As summarised in Table 1, it was seen that the higher the nano hBN content, the higher  $T_{onset}$  and  $T_{max}$  of the composites, thus better thermal

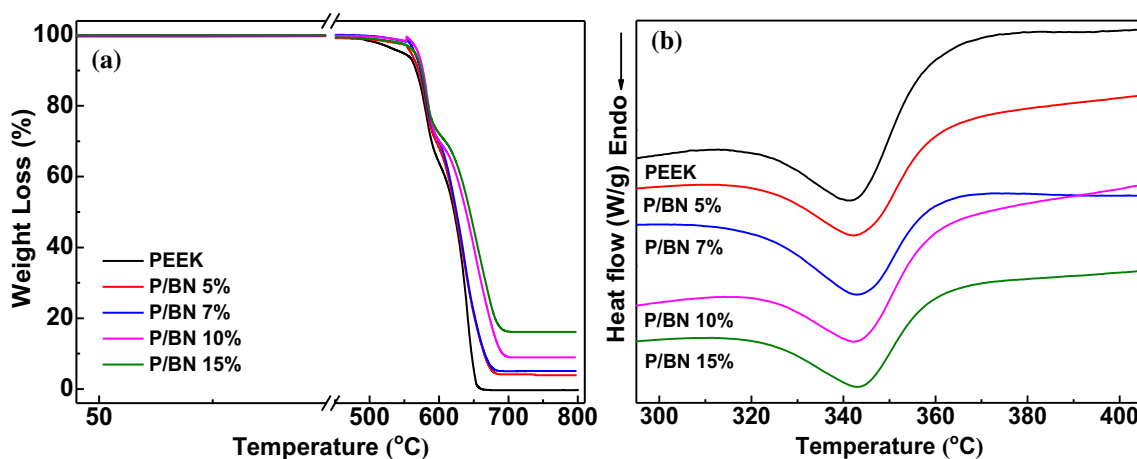


**Figure 2** **a** TGA curves and **b** DSC curves around the melting point of pure PEEK and the PEEK/hBN composites with different hBN loadings.

**Table 1** Thermal parameters obtained from DSC and TGA measurements of pure PEEK and PEEK/hBN composites at different hBN loadings ( $\sim 70$  nm)

Sample	Melting temperature $T_m$ (°C)	Melting enthalpy $\Delta H_m$ (J g <sup>-1</sup> )	Degree of crystallinity $X_c$ (%)	$T_{onset}$ (°C)	$T_{max}$ (°C)
PEEK	342.7	36.3	27.9	489	655
PEEK/hBN 5%	343.2	41.0	31.5	546	667
PEEK/hBN 7%	343.3	41.4	31.8	555	670
PEEK/hBN 10%	343.4	43.2	33.2	561	685
PEEK/hBN 15%	344.1	45.2	34.7	565	687

stability was obtained. A maximum increment of 32 °C in thermal degradation temperature ( $T_{max}$ ) was obtained with only 15 wt% of nano hBN filled PEEK composites. The increase in thermal stability of PEEK/hBN composites is due to the interfacial bonding between the matrix and the nanoparticles, which hinders the movement of the polymer chains [40]. Crystallization behaviour of pure PEEK and its composites was analyzed by differential scanning calorimetry and the key parameters are also given in Table 1. It was observed that the melting temperature ( $T_m$ ) and melting enthalpy ( $\Delta H_m$ ) of the composites increased with the increase in nano hBN content. The enthalpy of pure PEEK was about 36.3 J g<sup>-1</sup>, while the values were gradually increased with the increase in nano hBN loadings. A maximum increment of 25% in melting enthalpy was obtained with only 15 wt% nano hBN filled PEEK composites. This enhancement in enthalpy indicated an improved composite

crystallinity, which was estimated from the following equation [41]:

$$\text{Degree of crystallinity}(X_c) = \frac{\Delta H_m}{\Delta H_{m100\%}} \times 100 \quad (4)$$

where  $\Delta H_m$  is the melting enthalpy of the composites and  $\Delta H_{m100\%}$  is the melting enthalpy of a fully crystalline PEEK (130 J g<sup>-1</sup>) [42]. For pure PEEK,  $X_c$  was 27.9%, and this value was gradually increased with the addition of hBN nanoparticles. The composites with 15 wt% hBN showed  $X_c$  of 34.7%; thus 24% enhancement in  $X_c$  was obtained with respect to the pure PEEK matrix. This could be due to the heterogeneous nucleation effect of filler, which induces more nucleation sites in the crystal structure and reduces the nucleation energy with increasing nano hBN loadings [43]. This enhancement in the degree of crystallinity, i.e. the portion of the crystalline phase plays an important role on the thermal conductivity [44], which will be discussed in the following

section. The incorporation of hBN nanoparticles into PEEK matrix can also increase the  $T_g$  of the resulting composites which was obtained from DSC analysis. The neat polymer showed a glass transition at 145.1 °C and the  $T_g$  of the composites having 15 wt% hBN was 151.5 °C. The addition of hBN into the PEEK matrix, shifted  $T_g$  towards higher temperature, and the shifting degree depends on the interface interaction between nanoparticles and matrix. This increase in  $T_g$  with addition hBN nanoplatelets indicates the reduced mobility of the polymer chains after introducing the nanoparticles, which act as physical interlock points into the matrix [45].

Figure 3a shows the dimensional change as a function of temperature of pure PEEK and PEEK/hBN composites. The calculated CTE value is shown in Fig. 3b as a function of the hBN content. Aluminium was used as a calibrant. The CTE value for pure Al was 2.7  $\mu\text{m}/\text{mK}$ , which was slightly higher than the reported value (2.4  $\mu\text{m}/\text{mK}$ ). The CTE value gradually decreased with the increase in nano hBN content into the matrix (Fig. 3b). The lowest achieved CTE was 2.1  $\mu\text{m m}^{-1} \text{K}^{-1}$  at 30 wt% hBN content. A maximum of 62% decrease in CTE was observed in PEEK/hBN composites with 30 wt% hBN loadings. This reduction of CTE with the increasing hBN content is attributed due to the following reasons: (1) due to the increased hBN content, the volume fraction of the PEEK in the composite decreases; (2) as the hBN content increases, the average interparticle distance decreases and the polymer chain becomes so severe that it is progressively immobilized [46], and (3) the better dispersion of hBN nanofillers results in good interface bonding at the filler/matrix interface. The

intrinsic lower CTE of hBN (1.1–4.3  $\mu\text{m m}^{-1} \text{K}^{-1}$ ) may also reduce the CTE of the composites. The decrease in CTE indicates better dimensional stability of the composites as compared with the pure PEEK.

The thermal conductivity of the PEEK/hBN composites with different hBN loadings as a function of temperature is shown in Fig. 4a. The thermal conductivity of the composites was almost linear up to 250 °C, thus making it usable in high-temperature applications. The thermal conductivity of neat PEEK at 25 °C was 0.20  $\text{W m}^{-1} \text{K}^{-1}$ , while the composites showed much higher conductivity, which increased with the hBN content. The highest thermal conductivity achieved was 0.72  $\text{W m}^{-1} \text{K}^{-1}$  at 25 °C when 30 wt% hBN nanoparticles were incorporated into the PEEK matrix; thus, an enhancement of 242% in  $K$  was achieved with respect to pure PEEK. To further increase the conductivity, we have developed hybrid hBN (a mixture of 70 nm hBN and 500 nm hBN taken as 1:1 weight ratio) incorporated PEEK composites, and measured their thermal conductivities as a function of temperature are shown in Fig. 4b. In all three hBN loadings (10 wt%, 20 wt%, and 30 wt%), hybrid composites showed significant improvement in thermal conductivity over only single filler ( $\sim 70$  nm hBN) composites. The hybrid composites with 30 wt% total hBN loadings showed  $K$  value  $\sim 1.04 \text{ W m}^{-1} \text{K}^{-1}$ , an enhancement of 44% when compared to single filler composites at similar filler loadings. The improvement of thermal conductivity of a polymer composite depends not only on the filler properties, but also on the interaction between the polymer matrix and fillers. A better interaction results in the suppression of phonon

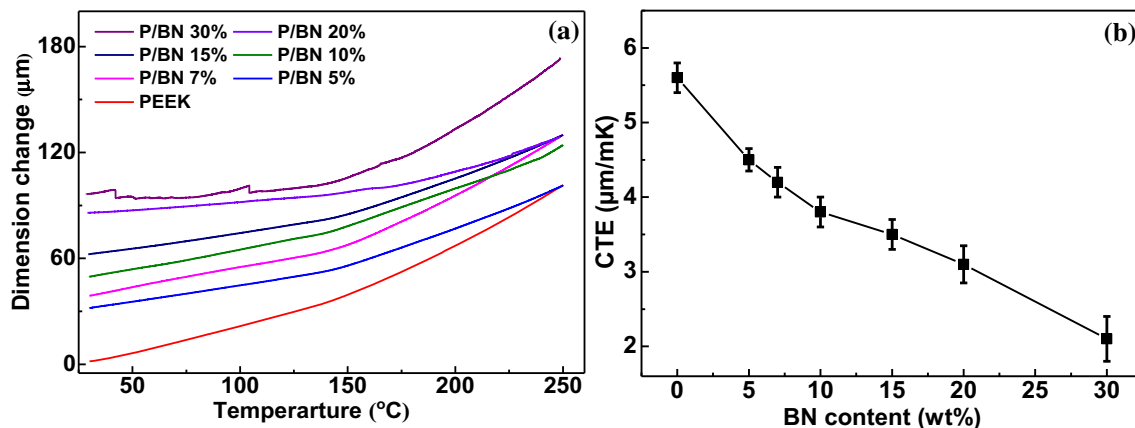


**Figure 3** **a** Dimensional change as a function of temperature and **b** CTE as a function of hBN content of pure PEEK and PEEK/hBN composites with different hBN loadings.

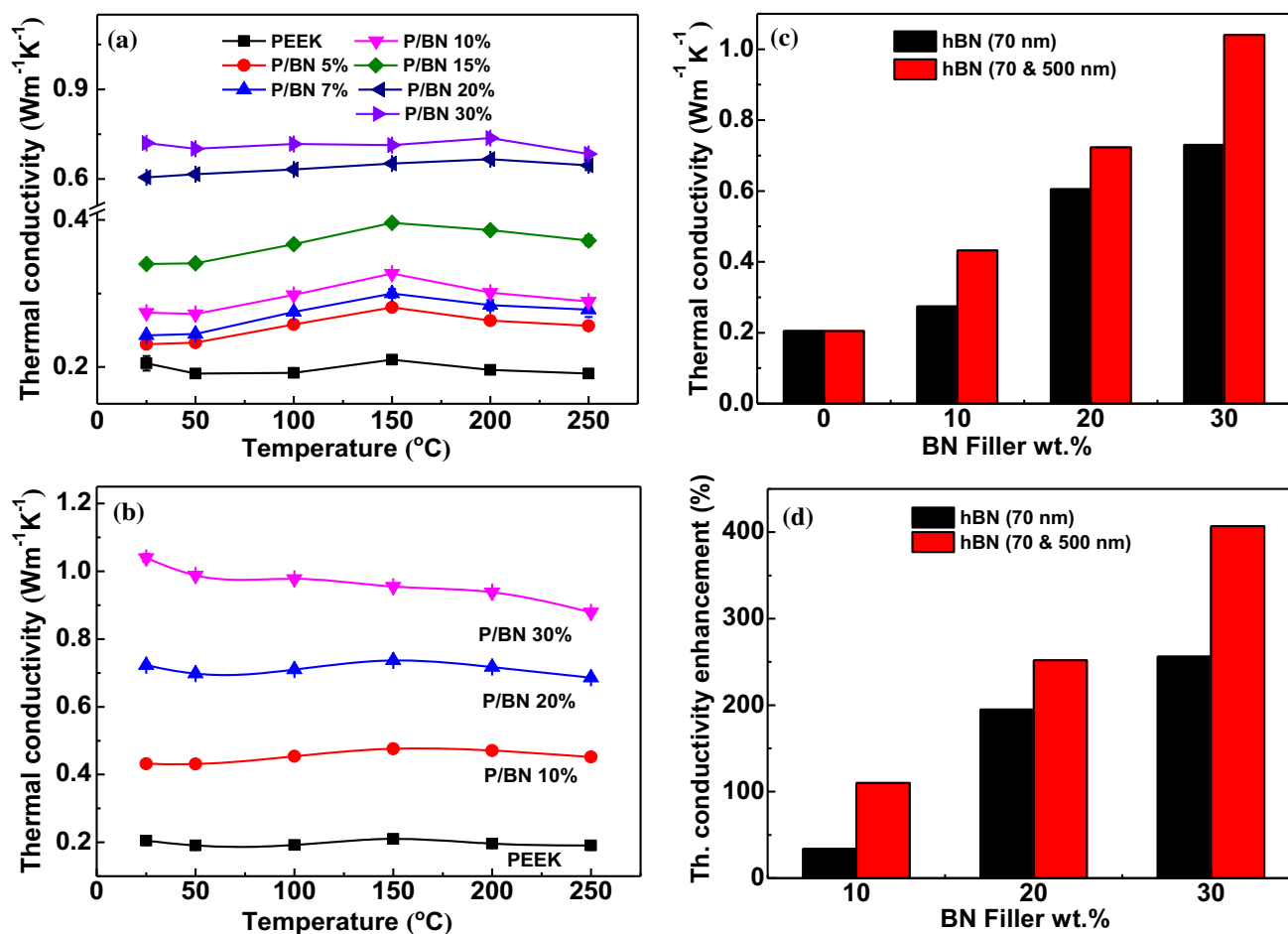


**Figure 4** Thermal conductivity of **a** 70 nm hBN incorporated PEEK composites, and **b** hybrid hBN (70 nm hBN and 500 nm hBN taken as 1:1 weight ratio) incorporated PEEK composites as a function of temperature. **c** Thermal conductivity and **d** the

scattering at the interfaces and thus, increase the conductivity. Also, filler size can affect the performance of the polymer composites. The decrease in the filler size significantly increases the surface-to-volume ratio which in turn increases the phonon scattering at the interfaces. Thus, the intrinsic thermal conductivity of fillers is one of many factors that contributes to the overall thermal conductivity of composites. Figure 4c shows the comparison of thermal conductivity at 25 °C between single filler (70 nm hBN) and hybrid filler reinforced PEEK composites from which a significant improvement in  $K$  was clearly observed in hybrid composites. The enhancement of  $K$  in case of hybrid composites over single sized hBN reinforced PEEK composites is shown in Fig. 4d. A maximum of 395% enhancement in  $K$  was obtained at 30 wt% hybrid composites,

enhancement in thermal conductivity as a function of total hBN loadings of pure PEEK and PEEK/hBN composites when using both 70 nm hBN and hybrid hBN.

whereas this value was 222% in case of single filler composites at similar loadings. This enhancement in thermal conductivity obtained in hybrid composites is due to the formation of enhanced filler network through the bridging of larger platelets by hBN nanoparticles. The synergistic effects between the hybrid fillers with different shapes and sizes were also explored by various researchers [31–36]. The formation of enhanced filler network through the bridging of hBN platelets in hybrid composites may also influence the interfacial phonon scattering and thermal resistance inside the composites. This was investigated by introducing the EMT model to calculate the interfacial thermal resistance ( $R_k$ ) between hBN and PEEK matrix.

Figure 5a, b show the fitting of experimental data of thermal conductivity based on EMT model for



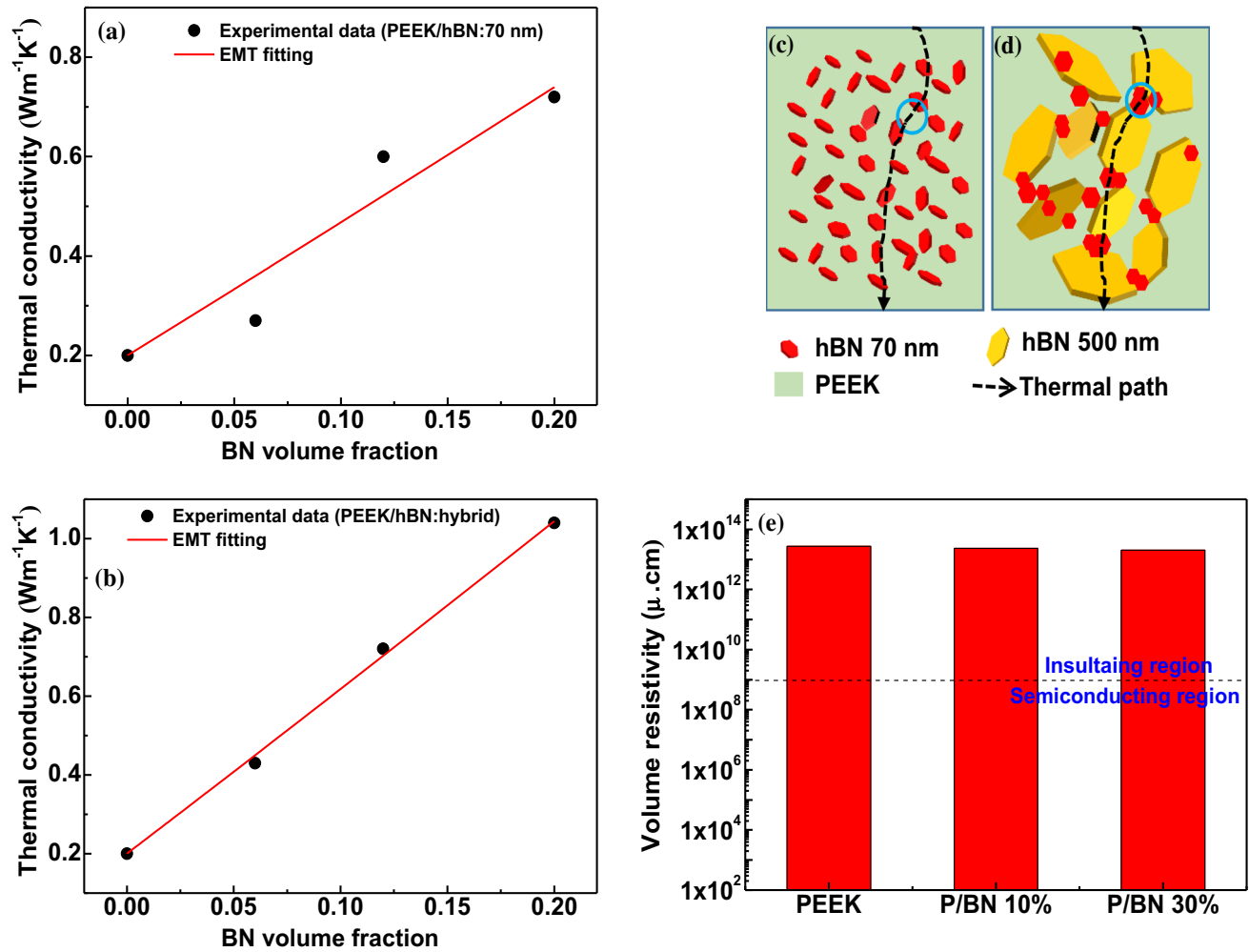


**Figure 5** Fitting of experimental data of thermal conductivity based on EMT model for **a** PEEK/hBN composites using 70 nm hBN and **b** PEEK/hBN composites using hybrid hBN. Formation of thermally conductive paths inside PEEK/hBN composite using **c** without inter-filler network (only 70 nm hBN) and **d** with inter-

filler network (hybrid fillers, i.e. 70 nm hBN and 500 nm hBN taken as 1:1 weight ratio). **e** Volume resistivity of pure PEEK and PEEK/hBN composite with two different hybrid hBN loadings: 10 wt% and 30 wt%.

PEEK/hBN composites (70 nm hBN) and PEEK/hBN hybrid composites. After fitting the experimental data of  $K$  according to Eq. (3), the  $R_k$  value was obtained from  $\beta_1$ . The  $R_k$  value in PEEK/hBN composites (for 70 nm hBN) was  $3.1 \times 10^{-8} \text{ m}^2 \text{ K W}^{-1}$ , whereas a lower interfacial thermal resistance ( $2.7 \times 10^{-8} \text{ m}^2 \text{ K W}^{-1}$ ) was obtained when using hybrid hBN fillers into PEEK matrix. This lower interfacial thermal resistance in PEEK/hBN hybrid composites results in higher thermal conductivity as evidenced in Fig. 4b, c, d. The effect of hybrid hBN fillers on the interfacial thermal resistance of the composites was further realized from the schematic, as shown in Fig. 5c, d. The hBN nanoplatelets act as thermal bridges to join the bigger particles and form

the inter-filler thermal network in the composites, as shown in Fig. 5d. As a consequence, PEEK/hBN hybrid composites with the inter-filler network (Fig. 5d) possess a higher thermal conductivity than those without an inter-filler network (Fig. 5c), because the inter-filler contact resistance is much less than the interfacial thermal resistance between matrix and filler.

The electrical insulation of the composites was evaluated by measuring the volume resistivity of the composites along with pure PEEK. All the PEEK/hBN hybrid composites exhibited a volume resistivity of  $\sim 10^{13} \Omega \text{ cm}$ , which is shown in Fig. 5e. No significant changes in volume resistivity were observed after increasing the hBN content (up to 30

wt%.) in the PEEK matrix or even in the single filler system. The measured volume resistivity is four orders of magnitude higher than the critical resistance for electrical insulation ( $10^9 \Omega \text{ cm}$ ). Thus, the developed composites demonstrate good potential in applications such as thermal management for power electronics, LED packaging, and other fields.

## Conclusions

PEEK/hBN composites have been fabricated by liquid mixing, and re-melting technique and after that their microstructure and thermal properties have been investigated. The X-ray diffraction studies indicated that PEEK structure was unchanged with the addition of hBN nanoparticles. The distribution of fillers into the PEEK was studied by scanning electron microscopy. The crystallinity of the composites increased with the addition of hBN nanoparticles into the PEEK matrix, which is due to heterogeneous nucleation effect of filler that induces more nucleation sites in the crystal structure hBN loadings. The mobility of the polymer chain was reduced after introducing the hBN nanoparticles, indicated by the increase in  $T_g$ . The lowest achieved CTE was  $2.1 \mu\text{m m}^{-1} \text{K}^{-1}$ , and the highest thermal conductivity was  $1.04 \text{ W m}^{-1} \text{K}^{-1}$  in PEEK/hBN composites at 30 wt% hybrid hBN content, due to the formation of thermally conductive inter-filler networks with reduced interfacial thermal resistance, which was confirmed from the EMT model. These improved thermal properties and good electrical insulation of the PEEK/hBN composites will expand its applications in thermal management.

## Acknowledgements

This work was supported by the feasibility study funded by the Engineering and Physical Sciences Research Council challenge network in automotive power electronics (Project No: EP/P00136X/1). The authors would like to gratefully acknowledge the Nanoscale and Microscale Research Centre at the University of Nottingham for SEM access, which was supported in part by the Engineering and Physical Sciences Research Council (Grant number EP/L022494/1). BG also wishes to acknowledge the

support from the University of Nottingham, Propulsion Futures Beacon project (Grant no: PF016).

## Compliance with ethical standards

**Conflict of interest** The authors declare no competing financial interest.

**Open Access** This article is licensed under a Creative Commons Attribution 4.0 International License, which permits use, sharing, adaptation, distribution and reproduction in any medium or format, as long as you give appropriate credit to the original author(s) and the source, provide a link to the Creative Commons licence, and indicate if changes were made. The images or other third party material in this article are included in the article's Creative Commons licence, unless indicated otherwise in a credit line to the material. If material is not included in the article's Creative Commons licence and your intended use is not permitted by statutory regulation or exceeds the permitted use, you will need to obtain permission directly from the copyright holder. To view a copy of this licence, visit <http://creativecommons.org/licenses/by/4.0/>.

## References

- [1] Dušek K, Rudajevova A (2017) Influence of latent heat released from solder joints II: PCB deformation during reflow and pad cratering defects. *J Mater Sci Mater Electron* 28:1070–1077
- [2] Hutapea P, Grenestedt JL (2003) Effect of temperature on elastic properties of woven-glass epoxy composites for printed circuit board applications. *J Electron Mater* 32:221–227
- [3] Mu M, Wan C, McNally T (2017) Thermal conductivity of 2D nano-structured graphitic materials and their composites with epoxy resins. *2D Mater* 4:042001. <https://doi.org/10.1088/2053-1583/aa7cd1>
- [4] Wen H, Zhang X, Xia R, Yang Z, Wu Y (2019) Thermodynamic simulations of SrTiO<sub>3</sub>/epoxy nanocomposites with different mass fractions. *SN Appl Sci* 1:354. <https://doi.org/10.1007/s42452-019-0363-1>
- [5] Wu Y, Zhang X, Negi A, He J, Hu G, Tian S, Liu J (2020) Synergistic effects of boron nitride (BN) nanosheets and silver (Ag) nanoparticles on thermal conductivity and electrical properties of epoxy nanocomposites. *Polymers* 12:426. <https://doi.org/10.3390/polym12020426>

- [6] Arif MF, Alhashmi H, Varadarajan KM, Koo JH, Hart AJ, Kumar S (2020) Multifunctional performance of carbon nanotubes and graphene nanoplatelets reinforced PEEK composites enabled via FFF additive manufacturing. *Compos B* 184:107625. <https://doi.org/10.1016/j.compositesb.2019.107625>
- [7] Huang X, Jiang P, Tanaka T (2011) A review of dielectric polymer composites with high thermal conductivity. *IEEE Electr Insul Mag* 27:8–16
- [8] Wang N, Yang Z, Thummavichai K, Xu F, Hu C, Chen H, Xia Y, Zhu Y (2017) Novel graphitic carbon coated IF-WS<sub>2</sub> reinforced poly(ether ether ketone) nanocomposites. *RSC Adv* 7:35265–35273
- [9] Zhou B, Ji X, Sheng Y, Wang L, Jiang Z (2004) Mechanical and thermal properties of poly-ether ether ketone reinforced with CaCO<sub>3</sub>. *Eur Polym J* 40:2357–2363
- [10] Rong C, Ma G, Zhang S, Song L, Chen Z, Wang G, Ajayan PM (2010) Effect of carbon nanotubes on the mechanical properties and crystallization behavior of poly(ether ether ketone). *Compos Sci Technol* 70:380–386
- [11] Goyal RK, Tiwari AN, Mulik UP, Negi YS (2007) Effect of aluminum nitride on thermomechanical properties of high-performance PEEK. *Compos A* 38:516–524
- [12] Lai YH, Kuo MC, Huang JC, Chen M (2007) On the PEEK composites reinforced by surface-modified nano-silica. *Mater Sci Eng* 458:158–169
- [13] Naffakh M, Diez-Pascual AM, Gomez-Fatou MA (2011) New hybrid nanocomposites containing carbon nanotubes, inorganic fullerene-like WS<sub>2</sub> nanoparticles and poly(ether ether ketone) (PEEK). *J Mater Chem* 21:7425–7433
- [14] Naffakh M, Diez-Pascual AM, Marco C, Gomez MA, Jimenez I (2010) Novel meltprocessable poly(ether ether ketone)(PEEK)/inorganic fullerene like WS<sub>2</sub> nanoparticles for critical applications. *J Phys Chem B* 114:11444–11453
- [15] Korzekwa J, Skoneczny W, Dercz G, Bara M (2014) Wear mechanism of Al<sub>2</sub>O<sub>3</sub>/WS<sub>2</sub> with PEEK/BG plastic. *J Tribol* 136:11601–11607
- [16] Puhan D, Bijwe J, Parida T, Trivedi P (2015) Investigations on performance properties of nano-micro composites based on polyetherketone, short carbon fibers and hexa-boron nitride. *Sci Adv Mater* 7:1002–1011
- [17] Denault J, Dumouchel M (1998) Consolidation process of PEEK/carbon composite for aerospace applications. *Adv Perform Mater* 5:83–96
- [18] Liu L, Xiao L, Li M, Zhang X, Chang Y, Shang L, Ao Y (2016) Effect of hexagonal boron nitride on high-performance polyether ether ketone composites. *Colloid Polym Sci* 294:127–133
- [19] Banerjee S, Kar KK (2017) Impact of degree of sulfonation on microstructure, thermal, thermomechanical and physicochemical properties of sulfonated poly ether ether ketone. *Polymer* 109:176–186
- [20] Banerjee S, Kar KK (2016) Superior water retention, ionic conductivity and thermal stability of sulfonated poly ether ether ketone/polypyrrole/aluminum phosphate nanocomposite-based polymer electrolyte membrane. *J Environ Chem Eng* 4:299–310
- [21] Banerjee S, Kar KK (2016) Synergistic effect of aluminium phosphate and tungstophosphoric acid on the physicochemical properties of sulfonated poly ether ether ketone nanocomposite membrane. *J Appl Polym Sci* 133:42952
- [22] Banerjee S, Kar KK, Ghorai MK, Das S (2014) Synthesis of polyether ether ketone membrane with pendent phosphonic acid group and determination of proton conductivity and thermal stability. *High Perform Polym* 27:402–411
- [23] Vadivelua MA, Ramesh Kumara C, Joshi GM (2016) Polymer composites for thermal management: a review. *Compos Interfaces* 23:847–872
- [24] Zeng H, Zhi C, Zhang Z, Wei X, Wang X, Guo W, Bando Y, Golberg D (2010) White graphemes: boron nitride nanoribbons via boron nitride nanotube unwrapping. *Nano Lett* 10:5049–5055
- [25] Terao T, Zhi C, Bando Y, Mitome M, Tang C, Golberg D (2010) Alignment of boron nitride nanotubes in polymeric composite films for thermal conductivity improvement. *J Phys Chem C* 114:4340–4344
- [26] Lin Y, Connell JW (2012) Advances in 2D boron nitride nanostructures: nanosheets, nanoribbons, nanomeshes, and hybrids with graphene. *Nanoscale* 4:6908–6939
- [27] Wang Z, Tang Z, Xue Q, Huang Y, Huang Y, Zhu M, Pei Z, Li H, Jiang H, Fu C, Zhi C (2016) Fabrication of boron nitride nanosheets by exfoliation. *Chem Rec* 16:1204–1215
- [28] Lindsay L, Broido DA (2011) Enhanced thermal conductivity and isotope effect in single-layer hexagonal boron nitride. *Phys Rev B* 84:155421. <https://doi.org/10.1103/PhysRevB.84.155421>
- [29] Lee GW, Park M, Kim J, Lee JI, Yoon HG (2006) Enhanced thermal conductivity of polymer composites filled with hybrid filler. *Compos A* 37:727–734
- [30] Guo Y, Ruan K, Shi X, Yang X, Gu J (2020) Factors affecting thermal conductivities of the polymers and polymer composites: a review. *Compos Sci Technol* 193:108134. <https://doi.org/10.1016/j.compscitech.2020.108134>
- [31] Gu J, Zhang Q, Dang J, Yin C, Chen S (2012) Preparation and properties of polystyrene/SiCw/SiCp thermal conductivity composites. *J Appl Polym Sci* 124:132–137
- [32] Li TL, Hsu SLC (2010) Enhanced thermal conductivity of polyimide films via a hybrid of micro- and nano-sized boron nitride. *J Phys Chem B* 114:6825–6829

- [33] Abbas Arani AA, Pourmoghdam F (2019) Experimental investigation of thermal conductivity behavior of MWCNTS- $\text{Al}_2\text{O}_3$ /ethylene glycol hybrid Nanofluid: providing new thermal conductivity correlation. *Heat Mass Transf* 55:2329–2339
- [34] Liu Z, Chen Z, Yu F (2019) Enhanced thermal conductivity of microencapsulated phase change materials based on graphene oxide and carbon nanotube hybrid filler. *Sol Energy Mater Sol Cells* 192:72–80
- [35] Owais M, Zhao J, Imani A, Wang GR, Zhang H, Zhang Z (2019) Synergetic effect of hybrid fillers of boron nitride, graphene nanoplatelets, and short carbon fibers for enhanced thermal conductivity and electrical resistivity of epoxy nanocomposites. *Compos A* 117:11–22
- [36] Zheng X, Kim S, Park CW (2019) Enhancement of thermal conductivity of carbon fiber-reinforced polymer composite with copper and boron nitride particles. *Compos A* 121:449–456
- [37] Akpan EI, Shen X, Wetzel B, Friedrich K (2019) Design and synthesis of polymer nanocomposites. *Polym Compos Funct Nanopar*. <https://doi.org/10.1016/b978-0-12-814064-2.00002-0>
- [38] Xu X, Hu R, Chen M, Dong J, Xiao B, Wang Q, Wang H (2020) 3D boron nitride foam filled epoxy composites with significantly enhanced thermal conductivity by a facial and scalable approach. *Chem Eng J* 397:125447. <https://doi.org/10.1016/j.cej.2020.125447>
- [39] Goyal RK, Tiwari AN, Mulik UP, Negi YS (2007) Novel high performance  $\text{Al}_2\text{O}_3$ /poly(ether ether ketone) nanocomposites for electronics applications. *Compos Sci Technol* 67:1802–1812
- [40] Goyal RK, Negi YS, Tiwari AN (2005) Preparation of high performance composites based on aluminum nitride/poly(ether-ether-ketone) and their properties. *Eur Polym J* 41:2034–2044
- [41] Ghosh B, Calderón RMT, González RE, Hevia SA (2017) Enhanced dielectric properties of PVDF/ $\text{CaCu}_3\text{Ti}_4\text{O}_{12}$ : Ag composite films. *Mater Chem Phys* 196:302–309
- [42] Kuo MC, Tsai CM, Huang JC, Chen M (2005) PEEK composites reinforced by nano-sized  $\text{SiO}_2$  and  $\text{Al}_2\text{O}_3$  particulates materials. *Mater Chem Phys* 90:185–195
- [43] Pan C, Zhang J, Kou K, Zhang Y, Wu G (2018) Investigation of the through-plane thermal conductivity of polymer composites with in-plane oriented hexagonal boron nitride. *Int J Heat Mass Transfer* 120:1–8
- [44] Zhou W, Zuo J, Ren W (2012) Thermal conductivity and dielectric properties of Al/PVDF composites. *Compos A* 43:658–664
- [45] Yu J, Huang X, Wu C, Wu X, Wang G, Jiang P (2012) Interfacial modification of boron nitride nanoplatelets for epoxy composites with improved thermal properties. *Polymer* 53:471–480
- [46] Tsagaropoulos G, Eisenberg A (1995) Dynamic mechanical study of the factors affecting the two-glass transition behavior of filled polymers: similarities and differences with random ionomers. *Macromolecules* 28:6067–6077

**Publisher's Note** Springer Nature remains neutral with regard to jurisdictional claims in published maps and institutional affiliations.